2021

Successional changes in carbon storage are sustained in a temperate forest across different initiating disturbances

Cameron Clay
Virginia Commonwealth University

Successional changes in carbon storage are sustained in a temperate forest across different initiating disturbances

A thesis submitted in partial fulfillment of the requirements for the degree of Master of Science at Virginia Commonwealth University.

by

Cameron Clay, B.S.

University of California, Davis (2017)

Director: Dr. Maria Rivera, PhD

Department of Biology

Virginia Commonwealth University

Richmond, Virginia

June, 2021

Acknowledgements

I would like to thank the incredible group of people who have supported me and helped make this project possible, and whose help is particularly commendable given the unique challenges provided by the Covid-19 pandemic over the course of the last year. I want to thank Dr. Christopher Gough, my PI and mentor, whose never ending supply of patience, wisdom, care, and thoughtful attention have provided the highest degree of support throughout my time in the program. I want to thank my fellow members of the Gough Lab, Jeff Atkins, Alley Barry, Maxim Grigri, Lisa Haber, Laura Hickey, Kayla Mathes, Kerstin Niedermaier and Ellen Stuart-Haëntjens, who have provided not only support in the field and lab, but also emotional support throughout these two years along with the wisdom, discussion and guidance necessary to collaboratively interpret the complicated natural processes that we observe as a group. I want to thank Dr. Christoph Vogel for his constant support with digital data sources, Dr. Luke Nave for his daily effort to create well-managed data sources and constant availability and presence when I needed help discussing, interpreting, and accessing data records, Dr. Peter Curtis for his support on understanding ecosystem model structure, Dr. Ben Bond-Lamberty for his support on creating effective code designs, and Dr. David Edwards for his consultation when designing the statistical analysis used for this project. I want to thank John Den Uyl and Brooke Propson for their guidance and explanation of the LTREB experimental design, and their hard work to gather field data taken during the notoriously difficult fall months at the University of Michigan Biological Station. I want to thank my entire committee, including Dr. Paul Bukaveckas and Dr. Rima Franklin, who have provided thought-provoking feedback that has helped lay the foundation for this work. And lastly, I want to thank my incredible friends and family who have always lent an ear and their time in an era where it has taken hard work to stay connected to each other.

Abstract

Managing forests for carbon (C) sequestration requires an understanding of how disturbance history shapes C pools and fluxes over successional time. At the University of Michigan Biological Station, we examined how two stand establishing disturbances influenced C pools and fluxes over 100+ years of succession, comparing these secondary forests with "legacy" late-successional stands encompassing ages and compositions that would be present in the absence of region-wide stand-replacing disturbance. Our work utilized measurements taken between 2014 and 2020 from separate experimental forest chronosequences initiated following clear-cut harvesting only or clear-cut harvesting and fire, along with three >130-yr-old late successional stands comprising deciduous broadleaf, evergreen needleleaf, and mixed forest functional types. Net primary production (NPP) was relatively similar regardless of stand age and establishing disturbance, averaging 4.95 Mg C ha^{-1} yr^{-1}, while heterotrophic soil respiration (R_{sh}) increased with age in the cut and burn chronosequence. The C pool and flux values of late successional stands varied by plant functional type, while total C pools averaged higher (271.78 Mg C ha^{-1}) than those of chronosequence stands (140.45 Mg C ha^{-1}). Estimates of net ecosystem balance varied depending on the approach used, with high and sometimes unrealistic R_{sh} values tipping net ecosystem production into C source territory, but temporally smoothed estimates of long-term C increment indicating instead that all chronosequence stands were C sinks. We conclude that late successional and old growth forests should be prioritized for protection and management, as they provide comparable C sequestration and superior storage to earlier successional forests and support a wide variety of other critical ecosystem services.

Vita

Cameron Clay was born on June 28th, 1995 in Orange, California. He graduated from San Dieguito Academy High School in Encinitas, California in 2013. He received his Bachelor of Science in Evolution, Ecology and Biodiversity from the University of California, Davis, in 2017, graduating with honors in the program for Research Scholars in Insect Biology. His publications include "Assessing the changes in *E. coli* levels and nutrient dynamics during vermicomposting of food waste under lab and field scale conditions" and "Artificial Light Increases Local Predator Abundance, Predation Rates, and Herbivory".

Introduction

Forests constitute a major terrestrial carbon (C) sink (Winjum et al 1992, Dixon et al. 1994), but dynamic patterns of disturbance and succession threaten the continued availability of this critical ecosystem service. In forests of the upper Great Lakes region, disturbances have largely shifted away from stand-replacing disturbances towards less severe partial disturbances, facilitating the broad regrowth of secondary forests (Wolter and White 2002). In the early 20th century, clear-cutting and, on occasion, subsequent slash-fueled fire reset ecological succession and led to the region-wide emergence of secondary forests with different compositional and structural features than their undisturbed late successional -- now "legacy" -- precursors (Gough et al. 2016; Curtis and Gough 2018). Comparisons of C pools and fluxes in secondary and late successional forests on the same landscape are rare, but critical to determining whether historical disturbances modified the region's terrestrial C sequestration potential and identifying which age structures sustain high rates of C uptake (Birdsey et al. 2006). Large scale, landscape-level studies also give insight into changes that may occur at the regional level, because they incorporate multiple ecosystems to give a more spatially extensive picture of changes occuring.

While quantitative comparisons are lacking, ecological theory, observations, and modeling all suggest that succession and disturbance shape trajectories of ecosystem C balance: the difference in C uptake and loss. Early theory posited that C uptake through net primary production (NPP) would initially outpace C losses from heterotrophic respiration (R_h) as young forests rapidly regrew with minimal competition and mortality (Kira and Shidei 1967, Odum 1969, Bormann and Likens 1979), but, as tree mortality increased with age, balanced NPP and R_h would result in ecosystem C neutrality. Decades of observations and modeling have since shown

that late successional forests can remain strong C sinks for centuries (Gough et al. 2016), but, like their younger counterparts, the C balance of older forests may vary because of differences in plant community composition, soils, and site productivity (Liu et al. 2018, Torn et al. 1997, Gough et al. 2019). Interacting with ecological succession, features of disturbance such as severity, frequency, and source affect the quantity and composition of material legacies such as biodiversity, seedling density, and nitrogen capital, all of which represent biotic and abiotic factors tied to rates and trajectories of NPP and R_h (LeBauer et al. 2008, Jannsens et al. 2010, Wales et al. 2020). Establishing an understanding of how the disturbance which establishes a secondary ecosystem affects long-term successional dynamics is essential to updating generalized theories about age-ecosystem C balance relationships, and to interpreting the breadth of successional patterns observed in nature (Corman et al. 2019). Consequently, experiments that address the interacting effects of disturbance and succession on forest C pools and fluxes are critical to informing management and policy aimed at sustaining the terrestrial C sink.

The difficulty of accurately quantifying belowground components of the C cycle has limited the production of high-confidence measures of net ecosystem C storage. R_h has been particularly difficult to study, as soil and surface microbes rely heavily on the carbon flux of surrounding surfaces and organisms to feed their processes. Several methods, including deep trenching, a method for segregating soil heterotrophs from autotrophic carbon, and the use of flux towers to measure total C flux, have previously converged on similar values, which allows for some confidence in capturing these more elusive components of forest C production (Bond-Lamberty et al. 2004, Bond-Lamberty et al. 2011, Hopkins et al. 2013). Our study focuses on utilizing measurements of R_h via the use of deep trenching, along with comparisons of long

term change in soil C pools, as the primary manner of elucidating this difficult to measure component of the C cycle.

We examined forest C pools and fluxes over 100 years of succession following two different establishing disturbances, and we compared these secondary forests with late successional legacy forests spanning three plant community functional types that would presently occupy the region's landscape in the absence of widespread stand-replacing disturbance. Our study included two experimental chronosequences initiated by stand-replacing clear-cutting or clear-cutting and fire within the last century, and three late successional mixed, deciduous broadleaf, and evergreen needleleaf forests averaging >150 years-old. Our objectives were to: 1) identify whether 100-yr successional changes in C pools and fluxes differ as a function of establishing disturbance; 2) characterize successional changes in C pools and fluxes following two different stand initiating disturbance; and 3) compare the magnitude of C pools and fluxes, including total C balance, in secondary and legacy forests. We hypothesized that 1) establishing disturbance would have a significant effect on long term carbon storage trajectory, with the clear-cut and burned site suppressed in its recovery of NPP; 2) establishing disturbance would have a significant effect on carbon pool and flux sizes, with every stage of the clear cut and burned site having lower overall sequestration values than its corresponding point on the clear-cut chronosequence trajectory; and 3) that legacy forests would be comparable or greater in their overall C pool and flux sizes to either of the secondary forest chronosequences, driven by relatively high NPP and low R_h values.

Methods

Study site

Our study site is located at the University of Michigan Biological Station near Pellston, Michigan (MI), in the northern Lower Peninsula. The forests that dominate this region are made up primarily of bigtooth aspen (*Populus grandidentata)*, paper birch (*Betula papyrifera*), white pine (*Pinus strobus*), red pine (*Pinus resinosa*), American beech (*Fagus grandifolia*), red maple (*Acer rubrum*), northern red oak (*Quercus rubra*), trembling aspen (*Populus tremuloides*), balsam fir (*Abies balsamea*) and sugar maple (*Acer saccharum*). The majority of the forests in the region are secondary forests recovering from widespread logging and subsequent burning that occurred in the late 19th and early 20th centuries. Soils are well drained, and made up primarily of sand (92%). The mean annual temperature is 5.5 ^{o}C and the mean annual precipitation is 817 mm. The growing season (i.e., the period from green-up to leaf-off) typically lasts around 120 days from approximately mid-May to early September (Curtis et al. 2005).

Our study sites encompass three disturbance histories: two forest chronosequences initiated following either i. stand-replacing clear-cutting (hereafter the "Cut Only" chronosequence) or ii. stand-replacing clearcutting and fire (hereafter the "Cut and Burn" chronosequence), and three late successional "legacy" stands representative of vegetation communities and structures that would have emerged more broadly in the absence of region-wide stand-replacing disturbance. The "Cut and Burn" chronosequence consists of four ~1 ha stands that were experimentally clear-cut harvested and burned in 1936, 1954, 1980, or 1998. An additional plot, cut and burned in 2017, was used only for heterotrophic respiration measurements, as other routine C pools and flux measurements have not yet been established. The "Cut Only" chronosequence consists of four, 0.4 to 1 ha stands that were clear cut in 1911, 1952, 1972, or 1987. In both chronosequences

and within each stand, measurements were conducted in 2 to 3 circular or rectangular 0.1 ha plots. In the case of the 1998 plot, one rectangular 0.06 ha plot and one rectangular 0.14 ha plot was used. Within each plot, a metal pole was placed at the plot center, and all measurements were made with reference to this center point along with cardinal directions. In the case of the 1998 plot, measurements are made relative to the NE corner of each plot.

Three late successional stands include: 1) a red pine dominated stand (hereafter "ENF", for Evergreen Needle-Leaf) established c. 1890; 2) a deciduous broadleaf dominated stand ("DBF" for Deciduous Broadleaf) established c. 1833; and 3) a mixed conifer-deciduous forest ("MIX") established c. 1891. Since experiment initiation in 2014, American beech, a dominant member of the canopy, has dramatically declined in the DBF stand (Atkins et al. 2020) due to widespread infection with beech bark disease, resulting in a substantial influx of detritus and canopy gap formation.

Soil respiration

To estimate the annual flux of CO_2 emitted from bulk soils and soil heterotrophs, we collected point measurements of total soil respiration (R_s) and heterotrophic soil respiration (R_{sh}), estimated continuous (i.e., gap-filled) fluxes from a temperature-response model, and integrated and scaled to the whole stand to derive annual fluxes. At azimuths of 0^o, 72^o, 144^o, 216^o, and 288^o, a 5 cm deep PVC soil collar was installed to a depth of 3 cm, at 3, 6, 9, 12, 15 m from plot center (respectively), to generate measurements of R_s. In early July 2020, we installed 80-cm deep trench collars constructed of schedule 40 PVC tube placed 1 m away from the 0^o, 144^o and 288^o shallow respiration collars within each subplot. Cores were driven vertically into the earth

using sledgehammers and wood pounding blocks until the core cleared the surface of the soil by approximately 3 cm. This method, also known as deep collar trenching, severs roots within the soil column, eliminating the flow of autotrophic respiration to that particular column of soil (Bond Lamberty et al. 2011). To ensure the isolation of R_{sh}, we measured paired surface and trenched collars every two days until trenched collars arrived at a low asymptote (Figure 1).

In situ R_{sh} and R_s were measured during four climatologically distinct periods between: July 28th and August 11th, 2020 (growing season); October 8th and 9th 2020; November 3rd and 4th; and November 16th and November 20th (off season). Measurements were taken using a LI-COR LI-6400 and a LI-6400-09 soil CO_2 flux chamber (LI-COR Inc.). When sampling each collar, we measured respiration twice to ensure stability. If the sequentially measured values differed by >10%, measurements were repeated until the values fell within 10% of each other. Concurrent with respiration, soil temperature measurements were taken 2 cm from the edge of each collar at a depth of 7 cm below the soil surface.

To scale R_s and R_{sh} from instantaneous point measurements to annual fluxes, we developed temperature response functions separately for R_s and R_{sh}. Two models were built to predict the relationship between temperature and soil respiration. For estimates during the offseason (days between day 281 of the year and day 365 and between day 1 and day 130), a linear model was designed for each plot using temperature as a predictor of R_s. For estimates during the growing season (days between day 131 and 280), a model of the form $\text{efflux} = a * e^{(b * \text{temperature})}$, where a and b are model specific parameters, was designed for each plot. We generated 30-minute continuous soil temperatures from regression models relating collar soil temperature to nearby continuous measurements from a fixed location. This location, the US-UMB Ameriflux tower, is located within 15 km of all sampled stands, and has taken continuous 30

minute interval soil temperature measurements since before 2008 (at a depth of 7.5 cm below the soil surface).

Using these 30 minute interval soil temperature estimates, 30 minute interval estimates of soil efflux were generated for the years 2014-2020. For offseason values, R_s was multiplied by the plot specific R_s:R_{sh} non-growing season ratio generated using the November respiration values. For growing season values, R_{sh} estimates were directly modeled using the exponential temperature response model. Values for each 30 minute interval were converted from mmol CO_2 m^{-2} s^{-1} (LI-COR Inc.) to Mg C ha^{-1} $30min^{-1}$. Values were then summed across the entire time period for each plot, and divided by 7 in order to generate annual measurements. Average values for each stand were generated using their component plot measurements. Values were expressed as negative fluxes.

Aboveground wood

A census of all trees larger than 8 cm diameter at breast height (dbh) within all plots was conducted in 2014 and 2019. All trees were previously tagged in order to identify each individual tree. Using diameter tapes, the dbh was measured to the nearest 0.1 cm for each individual tree.

To generate aboveground wood NPP (ΔM_a) values, all trees confirmed as alive in both 2014 and 2019 were selected. Biomass was generated for each tree for both 2014 and 2019 using species-specific two parameter allometries of the form $M_a = a(\text{dbh})^b$, using allometries generated on site and within the greater Midwest and Eastern United States regions (Wiant 1977, Ker 1980, Young et al. 1980, Schmitt and Grigal 1981, Crow and Erdmann 1983, Hocker and Early 1983, Perala and Alban 1994, Ter-Michaelian and Korzukhin, 1997). ΔM_a values were then generated

by calculating the difference between each tree's biomass in 2019 and 2014 and dividing by 5 to generate an annual value. If the dbh in a given tree was found to decrease by less than 10% within the 6 year interval, the individual tree was assumed to not have grown at all. For trees where a difference in dbh values was found to be a decrease of more than 10%, we assumed an error had occurred and the tree growth was replaced with the plot specific average of the growth rate of all individuals of its same species. Values were scaled to the hectare level and multiplied by the site specific mean tissue-weighted C fraction of live wood mass of 0.49 to convert from biomass to C mass (Gough et al. 2013).

To generate aboveground wood pool values (M_a), pools were calculated using dbh measurements taken in the 2019 census, using the same allometries used for ΔM_a. Values were then multiplied by 10 to get from 0.1 ha plot to 1 ha area (or, in the case of the uniquely sized 1998 plots, 16.66 or 7.14 to convert from 0.06 or 0.14, respectively), and multiplied by 0.50 to convert from biomass to C mass.

Belowground wood

Belowground wood pools (M_b) and Belowground wood NPP (ΔM_b) were calculated by multiplying corresponding plot-level aboveground wood values by 0.20 (Cairns et al. 1997).

Coarse woody debris

A census of coarse woody debris (pieces of debris with length > 20 cm and diameter > 5 cm) was conducted in 2014 and 2020. Debris was measured in 3 - 6m x 6m permanent subplots within

each plot, which were located at 0, 120 and 240 azimuths located 6 m from plot center. For each piece of debris measured, a diameter of both ends of the segment as well as the diameter of the midpoint were taken, for any length of a piece of debris which was above 5 cm diameter. Each piece of debris was assessed for degree of decomposition and assigned a value on a scale from 1-5, from being graded as wood that has recently fallen with intact bark and wood (1) to wood that has had its sapwood completely decay and bark missing and substantial heartwood missing (5) (Marra and Edmonds 1994). that has fully lost its cylindrical shape and was almost indistinguishable from the soil was not measured.

Coarse woody debris pool (M_{cwd}) values were calculated using the 2020 census. The volume was calculated by calculating an average diameter using the 3 diameters measured in the site, and then using those diameters (divided by two to get the radius) and the length of the piece to calculate the volume of a cylinder using the formula V = pi * (r^2) * h . Based on their level of decay recorded in the field, the volume of the piece was multiplied by a species-specific decay class value (Gough et al. 2007). These density metrics range from 0.06 kg/unit volume for level 5 decay pine samples up to 0.80 kg/unit volume for level 1 decay beech samples. To scale to Mg C on a per-plot basis, we multiplied by 92.592 (to convert from 108 meters in a given set of 3 subplots to a hectare), by 0.001 (to go from kg to Mg), and by 0.5 (to go from biomass to Mg C). The plot was used as the sampling unit (averaged across the 3 subplots within a plot), and means for the stand level were generated by averaging across plots.

Annual coarse woody debris fluxes (ΔM_{cwd}) were calculated using the same measurement techniques as M_{cwd}, except that annual values were gathered by subtracting each plot level value for 2014 from the plot value for 2020, and dividing by 6 to generate an annual flux estimate.

Fine root production

For fine root production measurements (ΔM_{fr}), ingrowth cores were used to measure the mass of roots that grew into root-free soil in a given growing season. The ingrowth cores consist of a 5.34 cm diameter, 35 cm long mesh tube with a disk of plastic mesh sewn onto the bottom. Each plot in a given stand had 2-5 cores installed, with ingrowth cores placed 5, 10, and 15 m out along transects at 0, 120, and 240 degrees from plot center. Each year, soils were collected from each plot in which the ingrowth cores would be installed by removing the combined A horizon from a 225 cm^2 area at the each installation location, coring out two 15 cm deep increments in the soil, and bringing these back to the lab for sieving (separately as A, 0-15, and 15-30 cm depth increments). Sieving was conducted using a 4 mm mesh within 2 days and removed rocks, coarse roots and most fine roots. Soils were then placed into each ingrowth core in order to reconstitute their morphology at the plot level, in which the 15 cm increments were removed, and deployed into the holes from which their material had been removed, within 4 days of initial soil collection. The O horizon, previously brushed away before removing the A horizon and coring the mineral soil depth increments, was placed back on top of the soil, and roots were allowed to incubate from late April/early May to late September/mid October, depending on the weather of the year (one full growing season). Incubations were taken every year between 2016 and 2019 in most plots.

Once incubation was complete, each core was removed and taken back to the lab and frozen, then later individually sorted. Technicians sorted fine roots by dumping the entire core into a 2mm sieve, hand picking and sieving out fine roots, and attempting to clean them of attached sand and silt as much as possible. Samples were adjusted for mineral contamination by

the use of CN and isotope analyses in 2016 and 2017, and by the use of a loss on ignition method for 2018 and 2019. Specifically, fine root biomass values were adjusted assuming an average C concentration of 47%, such that each fine root biomass value was scaled down in proportion to its amount of mineral contamination relative to the 47 %C 'clean' criterion. For loss on ignition, mass losses were multiplied by 0.5, assuming half the lost mass was C, to determine %C for each sample (Nave et al. 2020). Each plot was scaled to Mg C ha^{-1} based on the surface area and quantity of cores present.

Soil C mass and fine root standing stock

To calculate soil C mass, (M_s), we collected 3 soil profiles in each plot over the course of two days in July 2014. O and A horizons were removed together as a monolith, using a template with an area of 225 cm^2. Next, the mineral soil (M_{smin}) was removed using a 5.2 cm internal diameter steel pipe, in increments of 0-15, 15-30, 30-60, and 60-100 cm.

After the sampling was completed, the O + A monolith was immediately frozen, and processed over the course of the following 4 months. Mineral soil increments were air dried at 25°C for 1 week, then sieved to separate into pebbles/gravel (minerals >2mm), coarse root (roots > 2mm diameter), fine root (roots < 2mm diameter) and fine earth components. All fractions were then oven dried and weighed. The same process was followed in the O+A horizon monolith after fibrous organic material was removed from the top. After drying, fine root samples, fibrous organic material and fine earth were ball milled.

O and A horizons (M_{so}) and fine roots were analyzed for total C concentrations on a Costech Analytical CHN Analyzer in the UMBS Analytical Laboratory. Mineral soil C

concentrations for the 4 depth increments were determined on this instrument, a PerkinElmer Series II CHNS/O Elemental Analyzer, or both instruments. Total C concentrations for a random subset of n=10 samples (0.1 – 0.4 %C) analyzed on both instruments differed by 0.02 – 0.07 %C and were strongly related (r^2=0.981).

C stocks for the O + A horizon were calculated as the product of the mass of soil material per area, C concentration and correction for expansion factors (Nave et al. 2020). C stocks for mineral soils were calculated as the product of fine earth total C concentration, bulk density, and layer thickness. Bulk density values were calculated as the mass of fine earth divided by the volume of the sampled depth increment.

Leaf litter and fine debris

Leaf litter (M_l) and fine debris (M_{fd}) were collected annually between 2012 and 2020 via litter traps that were installed within all stands previous to the fall of 2012. These traps were constructed of window screen, made to be 1 m deep with a circular surface area of 0.264 m^2, and were supported at their opening by heavy gauge wire. They stand approximately 1 m above the ground on steel rods driven into the ground. Three traps were installed in most plots, although the number of traps per plot (and ultimately stand, which was the typical unit of replication) vary from year to year due to variable damage during the winter and growing season. Litter was collected every fall until litterfall ceased, then sorted into general fine litter and leaves. Values were scaled to Mg C per hectare by using the ratio of the total surface area of traps in a given stand to hectare, and by assuming a 48% C component of dry mass (Gough et al. 2007). Values were pooled at the stand level, and thus reported values here are universal across all plots within

a stand and represent averages across the 2012-2020 time frame. Litter traps were arranged randomly, with design varying from stand to stand. For presentation of values, leaf litter and fine debris were pooled and presented as leaf/litter C values (ΔM_{ll}), and given the high turnover of leaf and litter carbon, their pool and flux values are treated as synonymous.

Wood NPP

Total wood NPP (NPP_{wood}) and wood C Mass were calculated as the sum of above and belowground wood fluxes and pools, respectively:

$NPP_{wood} = \Delta M_a + \Delta M_b$

wood C Mass = $M_a + M_b$

Soil pools

Total soil C (M_s) was calculated as the sum of mineral (M_{smin}) and organic (M_{so}) soil layers:

$M_s = M_{msmin} + M_{so}$

Total C mass

Total C Mass was calculated as the sum of all C pool components:

Total C Mass = Wood C Mass + M_{ll} + M_{fr} + M_{cwd} + M_s

Net primary production

Net primary production (NPP) was calculated as the annual accumulation of above and belowground wood, fine litter, fine debris, as well as fine root production, and the addition of any coarse woody debris changes that were found to be positive:

$$NPP = NPP_{wood} + pos\Delta M_{cwd} + \Delta M_{fr} + M_{fd} + M_{ll}$$

Total heterotrophic respiration

Total heterotrophic respiration (R_h) was calculated as the sum of R_{sh} and any negative coarse woody debris changes:

$$R_h = | R_{sh}| + | neg\Delta M_{cwd}|$$

Net ecosystem production

Net ecosystem production, representing the net annual change of C mass in a given area and year, was calculated as:

$$NEP = NPP - R_h$$

Annual C increment

The annual C increment (ΔC), an alternative method to calculate total net change of C mass using changes in the size of major stable C pools (Gough et al. 2007), was also generated. As an example, the ΔC for the 1980 stand was calculated as:

$$\frac{(Wood\ C\ Mass(1980) + Ms(1980) + Mcwd(1980) - (Wood\ C\ Mass(1998) + Ms(1998) + Mcwd(1998)))}{18}$$

Statistical analysis

For all measurements except R_{sh}, standard errors were generated using plot as the sampling unit. Typically, if possible, plots were averaged, but for some measurements, such as the M_{ll} measurements, there were no plot level values, and thus no within stand replication exists. The standard errors of NPP_{wood}, Wood C Mass, R_h, NPP, NEP and ΔC were estimated as the quadratic sum of component errors (Gough et al. 2007).

For the heterotrophic respiration values, a 95% confidence interval was generated around the plot-specific parameters of the temperature and efflux models, and high and low model fits were generated using these two additional models. To test change across time, linear models were fitted to the chronosequence data points with time as the independent variable and the interaction of treatment and time as the dependent variable. If the treatment*time interaction was significant and the slope was non-zero, separate linear models were fit for the two different chronosequences. An alpha of 0.05 was used to determine statistical significance. To compare the chronosequence values to the late successional stand values, a one-way ANOVA was conducted using each of the two sets of chronosequence values and each late successional stand as 5 separate treatment groups. If significant, a post-hoc Tukey's HSD was run to identify which groups were statistically distinct.

Results

C pools

The total C Mass stored in biomass and soils increased similarly with stand age in the Cut Only and Cut and Burn chronosequences, and was greater but variable in late successional stands (Figure 2). Total C Mass increased on average from 105 Mg C ha^{-1} to 191 Mg C ha^{-1} over 87 years, averaging 184 Mg C ha^{-1} in the oldest chronosequence stands. The mean total C Mass of the chronosequence stands was lower than that of late successional stands, with DBF storing 355 Mg C ha^{-1} and ENF and MIX averaging 230 Mg C ha^{-1} . When individual biomass pools were considered, we found that Wood C Mass accumulated more rapidly over time in the Cut and Burn chronosequence than in the Cut Only chronosequence (Figure 3). Wood C Mass increased by 82 Mg C ha^{-1} over 62 years in the Cut and Burn chronosequence, while accumulating 53 Mg C ha^{-1} over the same amount of time in the Cut Only chronosequence. Late successional reference stands stored more in Wood C Mass than the chronosequence stands, with DBF exhibiting a high value of 241 Mg C ha^{-1}.

Soil C pools were similar among chronosequence and late successional stands, with the exception of greater M_{so} in two late successional stands (Figure 4). M_s, which was not significantly different over time or between the chronosequences and late successional stands, averaged 68.4 Mg C ha^{-1}. M_{smin} did not differ among stands, averaging 46.2 Mg C ha^{-1}. M_{so} averaged 25.7 Mg C ha^{-1} in the ENF and DBF late successional stands and was greater than the mean of 18.2 Mg C ha^{-1} in chronosequence and the MIX stands, but this quantity was not large enough to drive significant differences in M_s.

M_{cwd} was consistent between all treatments except for the late successional DBF stand (Figure 3), where the pool value of 25.13 Mg C ha^{-1} was nearly ten-fold larger than the next largest stand.

C fluxes

Heterotrophic respiration and coarse woody debris

R_{sh} increased over successional time in the Cut and Burn Chronosequence, increasing by 0.04 Mg C ha^{-1} yr^{-1} per year, but did not change over time in the Cut Only chronosequence. R_{sh} average values did not differ between chronosequences and late successional stands, averaging 7.24 Mg C ha^{-1} yr^{-1} (Figure 5). However, the estimated fraction of R_{sh} contributing to R_s was variable among stands and seasonally, ranging from a low of 35% in the 1952 Cut Only stand to a high of 76% in the late successional DBF stand during the growing season, and 47% in the late successional ENF and an implausible 109% of R_s in the 1952 stand during the dormant season.

ΔM_{cwd} was consistent between all treatments except for the DBF stand, in which the ΔM_{cwd} value of 3.11 Mg C ha^{-1} yr^{-1} represented an extremely large increase in coarse woody debris relative to all other stands. ΔM_{cwd} stand level values varied from being a mild source of C to a mild sink of C, with chronosequence stands averaging -0.015 Mg C ha^{-1} yr^{-1}.

Net primary production

Annual NPP varied by pool and, in some instances, among chronosequence and late successional stands (Figure 6). NPP_{wood} changes over time were not significant in either chronosequence, averaging 1.98 Mg C ha^{-1} yr^{-1}; however, NPP_{wood} was 1.64 Mg C ha^{-1} yr^{-1} greater in the DBF and 1.04 Mg C ha^{-1} yr^{-1} lower in ENF and MIX stands relative to the chronosequence mean. Fine Root NPP (ΔM_{fr}) showed no significant trends over time or among chronosequence and late

successional stands, averaging 1.68 Mg C ha^{-1} yr^{-1}. Leaf Litter and Fine Debris NPP (ΔM_{ll}) increased significantly over time in the Cut and Burn, but not the Cut Only, chronosequence, increasing by 36% over 50 years, while averaging 39% higher in the late successional stands.

Total NPP (Figure 6b) mirrored the trends of Wood NPP (Figure 6a), exhibiting no changes across successional time or between chronosequences, and variable among late successional stands Total NPP averaged 5.11 Mg C ha^{-1} yr^{-1} across the chronosequences and was greater in the DBF stand (6.53 Mg C ha^{-1} yr^{-1}) but lower in ENF (2.67 Mg C ha^{-1} yr^{-1}).

Net ecosystem production and C increment

The estimated net C balance of chronosequence and late successional stands differed substantially depending on the methodology used (i.e., NEP vs delta C based approaches). The ΔC approach produced estimates with very high uncertainty and which were not significantly different over stand age or between chronosequences, averaging 1.16 Mg C ha^{-1} yr^{-1} (Figure 7). NEP-based estimates of C balance also exhibited a high degree of uncertainty, suggesting the chronosequence, ENF, and MIX stands were moderate net C sources averaging - 2.34 Mg C ha^{-1} yr^{-1}. The exception was the DBF stand, which had an NEP value of 1.74 Mg C ha^{-1} yr^{-1}.

Discussion

Mean C pool and flux values in late successional stands were similar to or greater than those of regrown secondary forests, demonstrating that these older legacy forests sequester C at rates

comparable to younger forests. The larger C pool size of late successional forests was expected, as younger forests lag behind in the accumulation of C in biomass and O horizons (McGarvey 2015). However, comparable NPP and NEP in secondary and late successional forests is not aligned with theoretical expectations and some observations (Pregitzer and Euskirchen 2004). For example, our observations of sustained high NPP in the late successional stands are contrary to Odum's (1969) and Bormann and Likens's foundation successional theories and observations from other forests in the region (Bormann and Likens 1979), but they agree with more recent syntheses that found NPP was sustained in aging forests (Luyssaert et al. 2008, Gough et al. 2016). Our findings have important implications for forest management and the conservation of legacy late successional forests in the Upper Great Lakes region, suggesting that policies encouraging younger age structures, depending on the site conditions and ecology of a given site, may not be necessary to sustain the region C sink in plant biomass and may impair other critical ecosystem services supplied by older forests (Thompson et al. 2011).

Also contrasting with our hypothesis and theoretical expectations, fire prior to stand establishment had little effect on the successional trajectories or magnitude of C pools and fluxes. With the exception of more rapid increases in leaf NPP in the Cut and Burn stands and quantitatively small but significant differences in total C pools over time, fire was not a strong long-term modifier of the C cycle. This result is surprising because prior studies show the decades-long suppression of production that fire can have on some ecosystems (Hislop et al 2019). While fire may decrease N capital in the O-horizon (Nave et al 2011), annual atmospheric N deposition of 7.5 kg ha^{-1} yr^{-1} at our site represents a large fraction (15 %) of the total N requirement (Nave et al. 2009) and may have sufficiently replaced N lost during or immediately after fire. While severe fire may transition forests from C sinks to sources (Kashian et al. 2006),

material legacies, soil condition, climate and forest composition influence the extent and rate of recovery, which may range from years to decades (Burke et al. 1997, Gough et al. 2007, Shatford et al. 2007).

Our late successional forests represent ecosystems that may have been prevalent today in the absence of early 20th century clear-cut harvesting, providing clues into the degree of variation in C pools and fluxes that would be present if such forests had persisted. We observed substantial variability in NPP, from 2.67 Mg C ha^{-1} yr^{-1} to 6.53 Mg C $ha^{-1}yr^{-1}$, among late successional forests, that may be associated with soil, microclimatic conditions and differences in community composition, which are intertwined and their influence difficult to disentangle. Previous work at the same site demonstrated that the MIX stand had higher R_s values than the other late successional sites, suggesting that plant diversity may influence some of the C dynamics occurring on site (Liebman et al. 2017). Even so, all three late successional plant functional types continue to accumulate C in plant biomass, demonstrating that high rates of NPP are plausible in a range of older forests varying in site and compositional conditions. Our findings from a single forested landscape are consistent with cross-site syntheses showing different late successional forest types may sustain high rates of NPP (Luyssaert et al. 2008). Thus, our results and those of others reveal the degree to which older forests clearly have the potential to continue to store C in plant biomass, and thus should be prioritized for continued management (Luyssaert et al. 2008).

While heterotrophic soil respiration estimates derived from *in situ* measurements were higher than expected for our site and require further scrutiny, successional trends in the Cut and Burn chronosequence followed theoretical expectations of increasing respiration with age owing to higher detritus-fueled decomposition (Odum 1969, Harman 2010). Labile C in the form of leaf

litter and fine woody debris increased concurrently with R_{sh} in the Cut and Burn stand, suggesting successional changes in substrate supply may have fueled decomposition and that C inputs to the soil were roughly equivalent to efflux. Contrastingly, temporally stable leaf litter and fine and coarse woody debris in the Cut Only chronosequence may have limited successional changes in R_{sh}. Thus, disturbance type may impact the quantity of detritus supplied to the system, not just through death of large trees but through supply of leaf litter and fine debris.

Higher than expected in-situ R_{sh} rates, discrepancies between net C balance values (i.e. NEP vs. C increment), and large uncertainties in C pools and fluxes underscore several known limitations associated with inventory-based C balance estimation. Elevated, and sometimes impossibly high ($R_{sh} > R_s$) *in situ* heterotrophic respiration values resulted in NEP values that are much lower than observed in nearby stands using inventory and meteorological tower based approaches (Gough et al. 2007, 2008, 2013). With estimated heterotrophic respiration unrealistically exceeding total soil respiration in some instances, and overall annual R_h values higher than expected given the carbon inputs in this system, it is evident that some component of the C cycle is being over- or underestimated by our methodologies used, and thus close scrutiny of both our models and on-the-ground data is necessary. In contrast, mean C increment values of 1.16 Mg C ha^{-1} yr^{-1} in the chronosequence stands are comparable to independent estimates of NEP from our site and others in the region (Gough et al. 2007, 2008, 2013, Bond-Lamberty 2004). In situ estimates of R_{sh} and R_s, particularly when modeled and scaled, are sensitive to anomalous climate, statistical outliers, and oversimplification of a relatively complex ecosystem dynamic. Soil C and efflux are highly spatially variable across multiple ecosystem types including forests (Conant et al. 2003), and thus estimations of both these features via in situ measurements can be difficult, especially when taken over the course of only one calendar year.

Moreover, while chronosequences provide a uniquely powerful tool for viewing ecological change long periods of time through space-for-time substitution, caution must be taken when drawing inferences because of the lack of true treatment replication, changing environmental and atmospheric conditions over time, and potentially co-varying and thus confounding site and treatment factors (Bond-Lamberty et al. 2004). Our in situ R_{sh} estimates, derived from deep collar trenching, may have underrepresented the effects of root exudates and mycorrhizal production (Bond Lamberty et al. 2011). Given our anomalously high in situ R_{sh} values, future work leading to manuscript preparation will incorporate alternate estimates of this highly uncertain flux, derived independently from a mass balance approach (Giardina and Ryan 2002) and meta-regression based partitioning (Bond-Lamberty et al. 2004).

Conclusion

We conclude that late successional forests are capable of maintaining C pool and accrual values similar to those of earlier successional forests, with variation potentially depending heavily on the forest community composition. This demonstrates that legacy forests on the North American landscape could have served as large C sinks that compare in their substantiality to contemporary secondary forests, and thus the continued and improved preservation of old growth and late successional forest is justified for not only their biodiversity and cultural but also their C value. The two establishing disturbances examined in this study did not have large differences in their impacts on C storage or flux, with exceptions in certain components such as heterotrophic soil respiration, indicating that differences in disturbance history in secondary forests of the Upper Great Lakes region may not have a strong impact on C storage or flux. We recommend that future studies focus on deconstructing the mechanistic drivers of C flux and pool size, including developing a better understanding of what drives belowground C dynamics (be it microbial

dynamics, differences in abiotic soil conditions, etc.), determining the factors driving differences in C storage successional changes in different ecological communities, and working to refine methodologies for measuring ecosystem NEP, to allow for a multifaceted approach to better understand these dynamic ecosystem pools.

Literature Cited

Amiro, B. D., Barr, A. G., Barr, J. G., Black, T. A., Bracho, R., Brown, M., Chen, J., Clark, K. L., Davis, K. J., Desai, A. R., Dore, S., Engel, V., Fuentes, J. D., Goldstein, A. H., Goulden, M. L., Kolb, T. E., Lavigne, M. B., Law, B. E., Margolis, H. A., … Xiao, J. (2010). Ecosystem carbon dioxide fluxes after disturbance in forests of North America. *Journal of Geophysical Research: Biogeosciences*, *115*(4), 148–0227. https://doi.org/10.1029/2010JG001390

Atkins, J. W., Bond-Lamberty, B., Fahey, R. T., Haber, L. T., Stuart-Haëntjens, E., Hardiman, B. S., LaRue, E., McNeil, B. E., Orwig, D. A., Stovall, A. E. L., Tallant, J. M., Walter, J. A., & Gough, C. M. (2020). Application of multidimensional structural characterization to detect and describe moderate forest disturbance. *Ecosphere*, *11*(6), e03156. https://doi.org/10.1002/ecs2.3156

Birdsey, R., Pregitzer, K., & Lucier, A. (2006). Forest Carbon Management in the United States. *Journal of Environmental Quality*, *35*(4), 1461–1469. https://doi.org/10.2134/jeq2005.0162

Bormann, F. H., & Likens, G. E. (1979). Pattern and Process in a Forested Ecosystem. In *Pattern and Process in a Forested Ecosystem*. Springer New York. https://doi.org/10.1007/978-1-4612-6232-9

Bond-Lamberty, B., Wang, C., & Gower, S. T. (2004). Net primary production and net ecosystem production of a boreal black spruce wildfire chronosequence. *Global Change Biology*, *10*(4), 473–487. https://doi.org/10.1111/j.1529-8817.2003.0742.x

Bond-Lamberty, B., Bronson, D., Bladyka, E., & Gower, S. T. (2011). A comparison of trenched plot techniques for partitioning soil respiration. *Soil Biology and Biochemistry*, *43*(10), 2108–2114. https://doi.org/10.1016/j.soilbio.2011.06.011

Bowd, E. J., Banks, S. C., Strong, C. L., & Lindenmayer, D. B. (2019). Long-term impacts of wildfire and logging on forest soils. *Nature Geoscience*, *12*(2), 113–118. https://doi.org/10.1038/s41561-018-0294-2

Burke, R. A., Zepp, R. G., Tarr, M. A., Miller, W. L., & Stocks, B. J. (1997). Effect of fire on soil-atmosphere exchange of methane and carbon dioxide in Canadian boreal forest sites. *Journal of Geophysical Research Atmospheres*, *102*(24), 29289–29300. https://doi.org/10.1029/97jd01331

Cairns, M. A., Brown, S., Helmer, E. H., Baumgardner, G. A., Cairns, M. A., Brown, S., Helmer, E. H., & Baumgardner, G. A. (1997). Root biomass allocation in the world's upland forests. In *Oecologia* (Vol. 111, Issue 1±11). Springer-Verlag.

Caspersen, J. P., & Pacala, S. W. (2001). Successional diversity and forest ecosystem function. *Ecological Research*, *16*(5), 895–903. https://doi.org/10.1046/j.1440-1703.2001.00455.x

Certini, G. (2005). Effects of fire on properties of forest soils: A review. In *Oecologia* (Vol. 143, Issue 1, pp. 1–10). Springer. https://doi.org/10.1007/s00442-004-1788-8

Conant, R. T., Smith, G. R., & Paustian, K. (2003). Spatial Variability of Soil Carbon in Forested and Cultivated Sites. *Journal of Environmental Quality*, *32*(1), 278–286. https://doi.org/10.2134/jeq2003.2780

Cooper AW (1981) Above-ground biomass accumulation and net primary production during the first 70 years of succession in *Populus grandidentata* stands on poor sites in northern lower Michigan. In: *Forest Succession: Concepts and Application* (eds West DC, Shugart HH, Botkin DB), pp. 339-360. SPringer-Verlag, New York.

Corman, J. R., Collins, S. L., Cook, E. M., Dong, X., Gherardi, L. A., Grimm, N. B., Hale, R. L., Lin, T., Ramos, J., Reichmann, L. G., & Sala, O. E. (2019). Foundations and Frontiers of Ecosystem Science: Legacy of a Classic Paper (Odum 1969). *Ecosystems*, *22*(5), 1160–1172. https://doi.org/10.1007/s10021-018-0316-3

Costanza, R., Fisher, B., Mulder, K., Liu, S., & Christopher, T. (2007). Biodiversity and ecosystem services: A multi-scale empirical study of the relationship between species richness and net primary production. *Ecological Economics*, *61*(2–3), 478–491. https://doi.org/10.1016/j.ecolecon.2006.03.021

Crow TR, Erdmann GG (1983) *Weight and volume equations and tables for red maple in the Lake States.* US Forest Service Research Paper, NC-242, 14.

Curtis, P. S., & Gough, C. M. (2018). Forest aging, disturbance and the carbon cycle. In *New Phytologist* (Vol. 219, Issue 4, pp. 1188–1193). Blackwell Publishing Ltd. https://doi.org/10.1111/nph.15227

Dixon, R. K., Solomon, A. M., Brown, S., Houghton, R. A., Trexier, M. C., & Wisniewski, J. (1994). Carbon Pools and Flux of Global Forest Ecosystems. *Science*, *263*(5144), 185–190. https://doi.org/10.1126/science.263.5144.185

Dornelas, M. (2010). Disturbance and change in biodiversity. *Philosophical Transactions of the Royal Society B: Biological Sciences*, *365*(1558), 3719–3727

https://doi.org/10.1098/rstb.2010.0295

Giardina, C. P., & Ryan, M. G. (2002). Total belowground carbon allocation in a fast-growing Eucalyptus plantation estimated using a carbon balance approach. *Ecosystems*, *5*(5), 487–499. https://doi.org/10.1007/s10021-002-0130-8

Gough, C. M., Vogel, C. S., Harrold, K. H., George, K., & Curtis, P. S. (2007). The legacy of harvest and fire on ecosystem carbon storage in a north temperate forest. *Global Change Biology*, *13*(9), 1935–1949. https://doi.org/10.1111/j.1365-2486.2007.01406.x

Gough, C. M., Vogel, C. S., Schmid, H. P., & Curtis, P. S. (2008). Controls on annual forest carbon storage: Lessons from the past and predictions for the future. *BioScience*, *58*(7), 609–622. https://doi.org/10.1641/B580708

Gough, C. M., Hardiman, B. S., Nave, L. E., Bohrer, G., Maurer, K. D., Vogel, C. S., Nadelhoffer, K. J., & Curtis, P. S. (2013). Sustained carbon uptake and storage following moderate disturbance in a Great Lakes forest. *Ecological Applications*, *23*(5), 1202–1215. https://doi.org/10.1890/12-1554.1

Gough, C. M., Curtis, P. S., Hardiman, B. S., Scheuermann, C. M., & Bond-Lamberty, B. (2016). Disturbance, complexity, and succession of net ecosystem production in North America's temperate deciduous forests. *Ecosphere*, *7*(6), e01375. https://doi.org/10.1002/ecs2.1375

Gough, C. M., Atkins, J. W., Fahey, R. T., & Hardiman, B. S. (2019). High rates of primary production in structurally complex forests. *Ecology*, *100*(10), e02864. https://doi.org/10.1002/ecy.2864

Groffman, P.M., Baron, J.S., Blett, T. *et al.* Ecological Thresholds: The Key to Successful Environmental Management or an Important Concept with No Practical Application?. *Ecosystems* 9, 1–13 (2006). https://doi.org/10.1007/s10021-003-0142-z

Hardiman, B. S., Gough, C. M., Halperin, A., Hofmeister, K. L., Nave, L. E., Bohrer, G., & Curtis, P. S. (2013). Maintaining high rates of carbon storage in old forests: A mechanism linking canopy structure to forest function. *Forest Ecology and Management*, *298*, 111–119. https://doi.org/10.1016/j.foreco.2013.02.031

Hislop, S., Jones, S., Soto-Berelov, M., Skidmore, A., Haywood, A., & Nguyen, T. H. (2019). High fire disturbance in forests leads to longer recovery, but varies by forest type. *Remote Sensing in Ecology and Conservation*, *5*(4), 376–388. https://doi.org/10.1002/rse2.113

Hocker HW Jr, Early DJ (1983) Biomass and leaf area equations for northern forest species. *New Hampshire Agricultural Experiment Station University of New Hampshire Research Report,* 102, 27.

Hopkins, F., Gonzalez-Meler, M. A., Flower, C. E., Lynch, D. J., Czimczik, C., Tang, J., & Subke, J. A. (2013). Ecosystem-level controls on root-rhizosphere respiration. In *New*

Phytologist (Vol. 199, Issue 2, pp. 339–351). John Wiley & Sons, Ltd. https://doi.org/10.1111/nph.12271

Janssens, I. A., Dieleman, W., Luyssaert, S., Subke, J. A., Reichstein, M., Ceulemans, R., Ciais, P., Dolman, A. J., Grace, J., Matteucci, G., Papale, D., Piao, S. L., Schulze, E. D., Tang, J., & Law, B. E. (2010). Reduction of forest soil respiration in response to nitrogen deposition. In *Nature Geoscience* (Vol. 3, Issue 5, pp. 315–322). Nature Publishing Group. https://doi.org/10.1038/ngeo844

Kashian, D. M., Romme, W. H., Tinker, D. B., Turner, M. G., & Ryan, M. G. (2006). Carbon Storage on Landscapes with Stand-replacing Fires. *BioScience*, *56*(7), 598–606. https://doi.org/10.1641/0006-3568(2006)56[598:CSOLWS]2.0.CO;2

Ker, M. F. (1980). Tree biomass equations for seven species in southwestern New Brunswick. *Tree Biomass Equations for Seven Species in Southwestern New Brunswick.*, *No. M-X-114, 18*.

Kira, T., & Shidei, T. (1967). Primary production and turnover of organic matter in different forest ecosystems of the Western Pacific. Japanese Journal of Ecology, *17*(2), 70–87. https://doi.org/10.18960/seitai.17.2_70

Koerper G (1977) *The aboveground biomass and annual net production of bigtooth aspen (Populus grandidentata Michx.) on three soil types in northern lower Michigan.* MS Thesis, University of Michigan Ann Arbor, MI.

LeBauer, D. S., & Treseder, K. K. (2008). Nitrogen limitation of net primary productivity in terrestrial ecosystems is globally distributed. *Ecology*, *89*(2), 371–379. https://doi.org/10.1890/06-2057.1

Liebman, E., Yang, J., Nave, L. E., Nadelhoffer, K. J., & Gough, C. M. (2017). Research Article: Soil respiration in upper Great Lakes old-growth forest ecosystems. *BIOS*, *88*(3), 105–115. https://doi.org/10.1893/0005-3155-88.3.105

Liu, X., Trogisch, S., He, J. S., Niklaus, P. A., Bruelheide, H., Tang, Z., Erfmeier, A., Scherer-Lorenzen, M., Pietsch, K. A., Yang, B., Kühn, P., Scholten, T., Huang, Y., Wang, C., Staab, M., Leppert, K. N., Wirth, C., Schmid, B., & Ma, K. (2018). Tree species richness increases ecosystem carbon storage in subtropical forests. *Proceedings of the Royal Society B: Biological Sciences*, *285*(1885). https://doi.org/10.1098/rspb.2018.1240

Luyssaert, S., Schulze, E. D., Börner, A., Knohl, A., Hessenmöller, D., Law, B. E., Ciais, P., & Grace, J. (2008). Old-growth forests as global carbon sinks. *Nature*, *455*(7210), 213–215. https://doi.org/10.1038/nature07276

Marra, J. L., & Edmonds, R. L. (1994). Coarse woody debris and forest floor respiration in an old-growth coniferous forest on the Olympic Peninsula, Washington, USA. *Canadian Journal of Forest Research*, *24*(9), 1811–1817. https://doi.org/10.1139/x94-234

McGarvey, J. C., Thompson, J. R., Epstein, H. E., & Shugart, H. H. (2015). Carbon storage in old-growth forests of the Mid-Atlantic: Toward better understanding the eastern forest carbon sink. *Ecology*, *96*(2), 311–317. https://doi.org/10.1890/14-1154.1

Nave, L. E., Vance, E. D., Swanston, C. W., & Curtis, P. S. (2009). Impacts of elevated N inputs on north temperate forest soil C storage, C/N, and net N-mineralization. *Geoderma*, *153*(1–2), 231–240. https://doi.org/10.1016/j.geoderma.2009.08.012

Nave, L. E., Gough, C. M., Maurer, K. D., Bohrer, G., Hardiman, B. S., Le Moine, J., Munoz, A. B., Nadelhoffer, K. J., Sparks, J. P., Strahm, B. D., Vogel, C. S., & Curtis, P. S. (2011). Disturbance and the resilience of coupled carbon and nitrogen cycling in a north temperate forest. *Journal of Geophysical Research: Biogeosciences*, *116*(4), 4016. https://doi.org/10.1029/2011JG001758

Nave, L., K. Nadelhoffer, and C. Gough (2020). Forest tree, woody debris, and soil inventory data from long-term research plots for LTREB at the University of Michigan Biological Station ver 6. Environmental Data Initiative. https://doi.org/10.6073/pasta/400d6122fc25f0ab79ba2b63ca415bd4

Odum, E.P. (1969). The strategy of ecosystem development. *Science,* 164, 262-270.

Perala DA, Alban DH (1994) *Allometric biomass estimators for aspen-dominated ecosystems in the Upper Great Lakes.* US Department of Agriculture Forest SErvice Research Paper, NC-134, 38.

Peters, E. B., Wythers, K. R., Bradford, J. B., & Reich, P. B. (2013). Influence of Disturbance on Temperate Forest Productivity. *Ecosystems*, *16*(1), 95–110. https://doi.org/10.1007/s10021-012-9599-y

Pregitzer, K. S., & Euskirchen, E. S. (2004). Carbon cycling and storage in world forests: Biome patterns related to forest age. In *Global Change Biology* (Vol. 10, Issue 12, pp. 2052–2077). John Wiley & Sons, Ltd. https://doi.org/10.1111/j.1365-2486.2004.00866.x

Scheuermann, C. M., Nave, L. E., Fahey, R. T., Nadelhoffer, K. J., & Gough, C. M. (2018). Effects of canopy structure and species diversity on primary production in upper Great Lakes forests. *Oecologia*, *188*(2), 405–415. https://doi.org/10.1007/s00442-018-4236-x

Schmitt, M. D. C., & Grigal, D. F. (1981). Generalized biomass estimation equations for Betula papyrifera Marsh. . *Canadian Journal of Forest Research*, *11*(4), 837–840. https://doi.org/10.1139/x81-122

Shatford, J. P. A., Hibbs, D. E., & Puettmann, K. J. (2007). Conifer regeneration after forest fire in the Klamath-Siskiyous: How much, how soon? *Journal of Forestry*, *105*(3), 139–146. https://doi.org/10.1093/jof/105.3.139

Stuart-Haëntjens, E. J., Curtis, P. S., Fahey, R. T., Vogel, C. S., & Gough, C. M. (2015). Net primary production of a temperate deciduous forest exhibits a threshold response to

increasing disturbance severity. *Ecology*, *96*(9), 2478–2487. https://doi.org/10.1890/14-1810.1

Ter-Mikaelian, M. T., & Korzukhin, M. D. (1997). Biomass equations for sixty-five North American tree species. *Forest Ecology and Management*, *97*(1), 1–24. https://doi.org/10.1016/S0378-1127(97)00019-4

Thompson, I. D., Okabe, K., Tylianakis, J. M., Kumar, P., Brockerhoff, E. G., Schellhorn, N. A., Parrotta, J. A., & Nasi, R. (2011). Forest biodiversity and the delivery of Ecosystem goods and services: Translating science into Policy. *BioScience*, *61*(12), 972–981. https://doi.org/10.1525/bio.2011.61.12.7

Torn, M. S., Trumbore, S. E., Chadwick, O. A., Vitousek, P. M., & Hendricks, D. M. (1997). Mineral control of soil organic carbon storage and turnover. *Nature*, *389*(6647), 170–173. https://doi.org/10.1038/38260

Wales, S. B., Kreider, M. R., Atkins, J., Hulshof, C. M., Fahey, R. T., Nave, L. E., Nadelhoffer, K. J., & Gough, C. M. (2020). Stand age, disturbance history and the temporal stability of forest production. *Forest Ecology and Management*, *460*. https://doi.org/10.1016/j.foreco.2020.117865

White, L. L., Zak, D. R., & Barnes, B. V. (2004). Biomass accumulation and soil nitrogen availability in an 87-year-old Populus grandidentata chronosequence. *Forest Ecology and Management*, *191*(1–3), 121–127. https://doi.org/10.1016/j.foreco.2003.11.01

Wiant, H. V. (1977). Tables and procedures for estimating weights of some Appalachian hardwoods. In *West Virginia Agricultural and Forestry Experiment Station Bulletins*. 659, 36. https://doi.org/10.33915/agnic.65

Winjum, J. K., Dixon, R. K., & Schroeder, P. E. (1992). Estimating the global potential of forest and agroforest management practices to sequester carbon. *Water, Air, and Soil Pollution*, *64*(1), 213–227. https://doi.org/10.1007/BF00477103

Wolter, P. T., & White, M. A. (2002). Recent forest cover type transitions and landscape structural changes in northeast Minnesota, USA. *Landscape Ecology*, *17*(2), 133–155. https://doi.org/10.1023/A:1016522509857

Young, H. E., Ribe, J. H., & Wainwright, K. (1980). *Weight Tables for Tree and Shrub Species in Maine*. Life Sciences and Agriculture Experimental Station, University of Maine at Orono. Miscellaneous Report 230. 84 pp.

Appendix

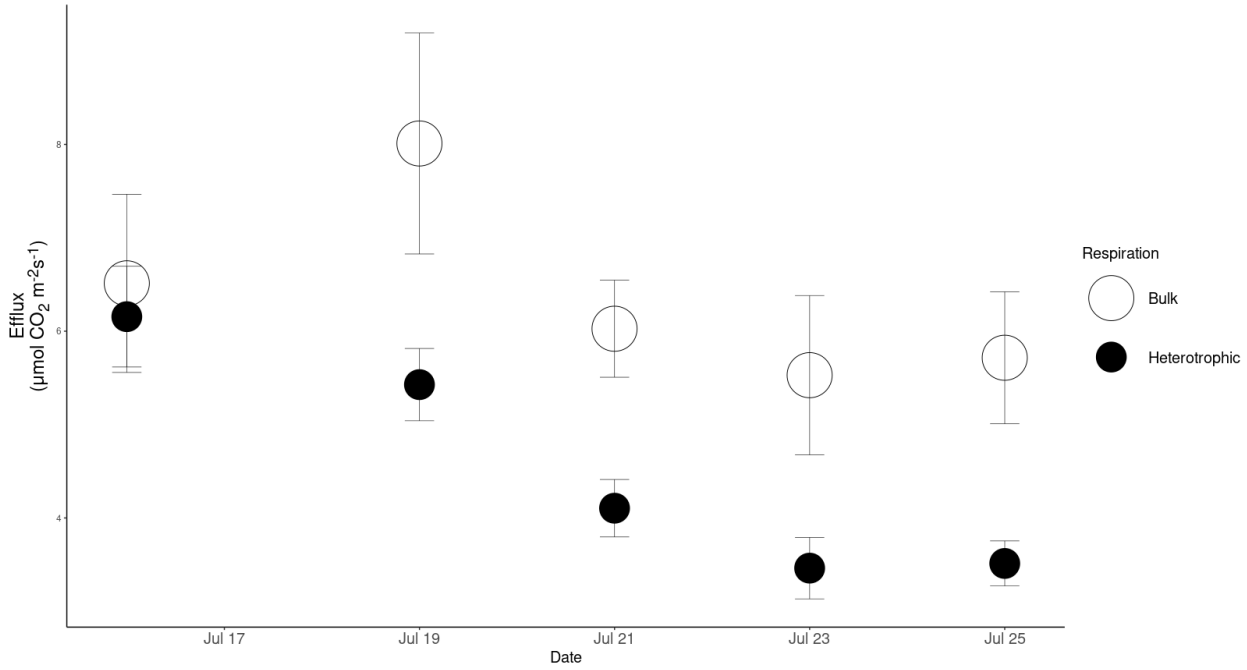

Figure 1: Soil efflux from a subset of bulk/heterotrophic point measurements, demonstrating the asymptotic decline of heterotrophic respiration over the course of approximately a week. Measurements taken during three weeks of July 2020. Error bars represent +/- SE.

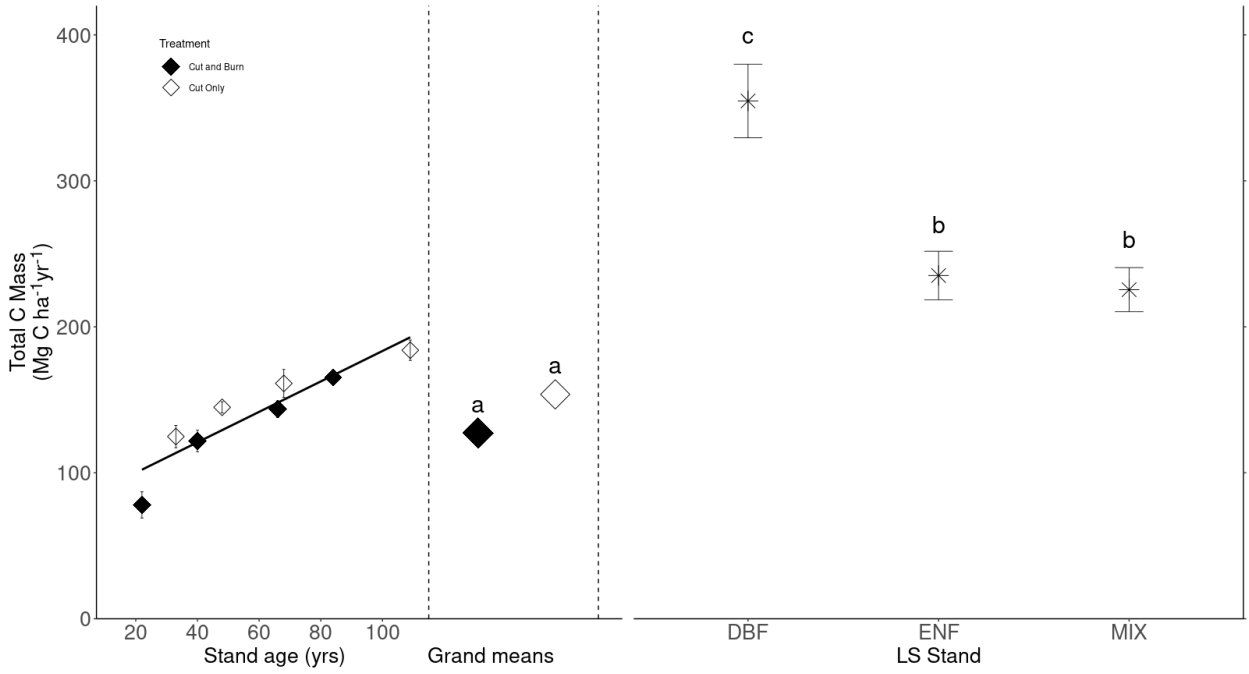

Figure 2: Total C Mass across stand age and late successional stands. Error bars represent +/- SE. Mean values with shared letters above them represent values that are statistically the same.

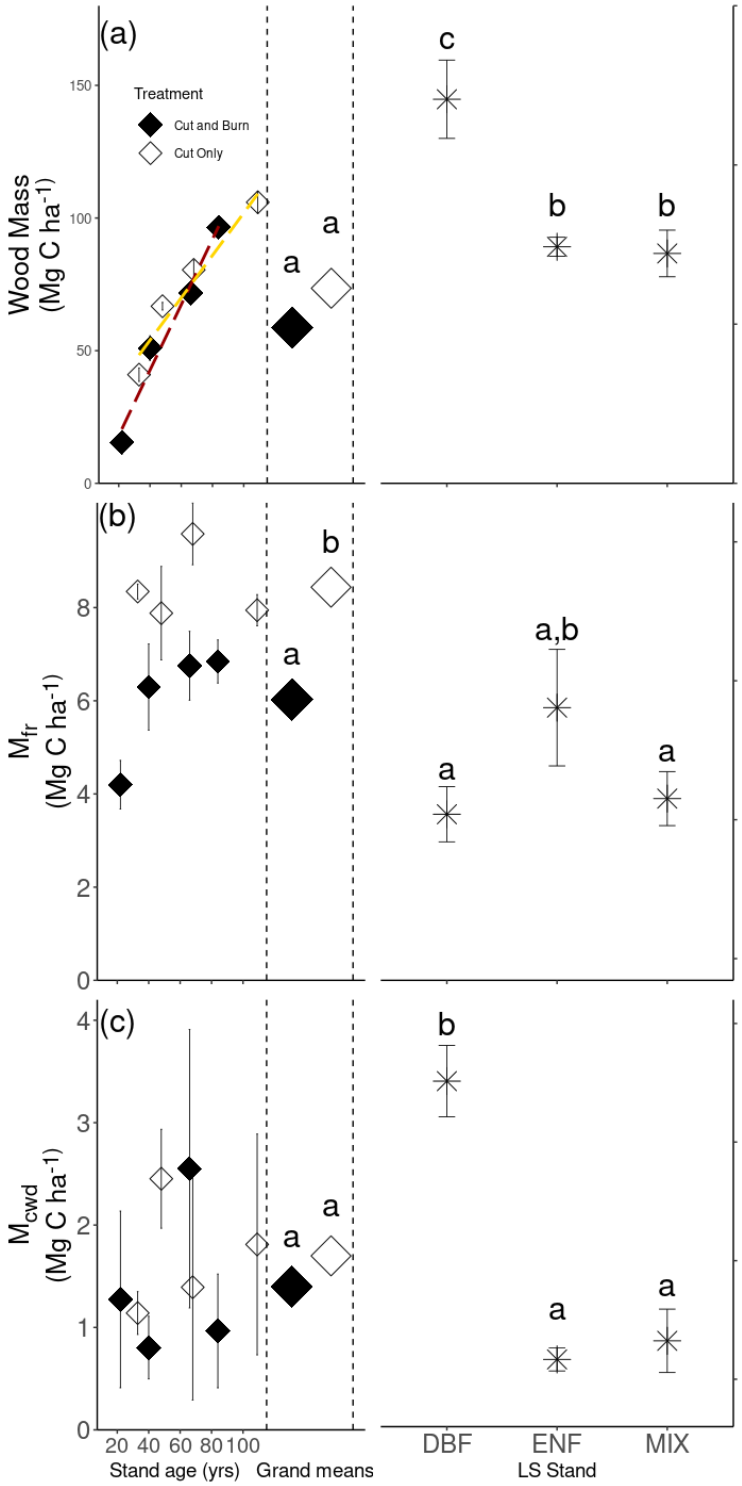

Figure 3. Carbon Mass of Wood, Fine Roots, and Coarse Woody Debris, across stand age and late successional stands. Red and yellow lines indicate non-zero trends that are statistically

significantly different from each other. Error bars represent +/- SE. Mean values with shared letters above them represent values that are statistically the same.

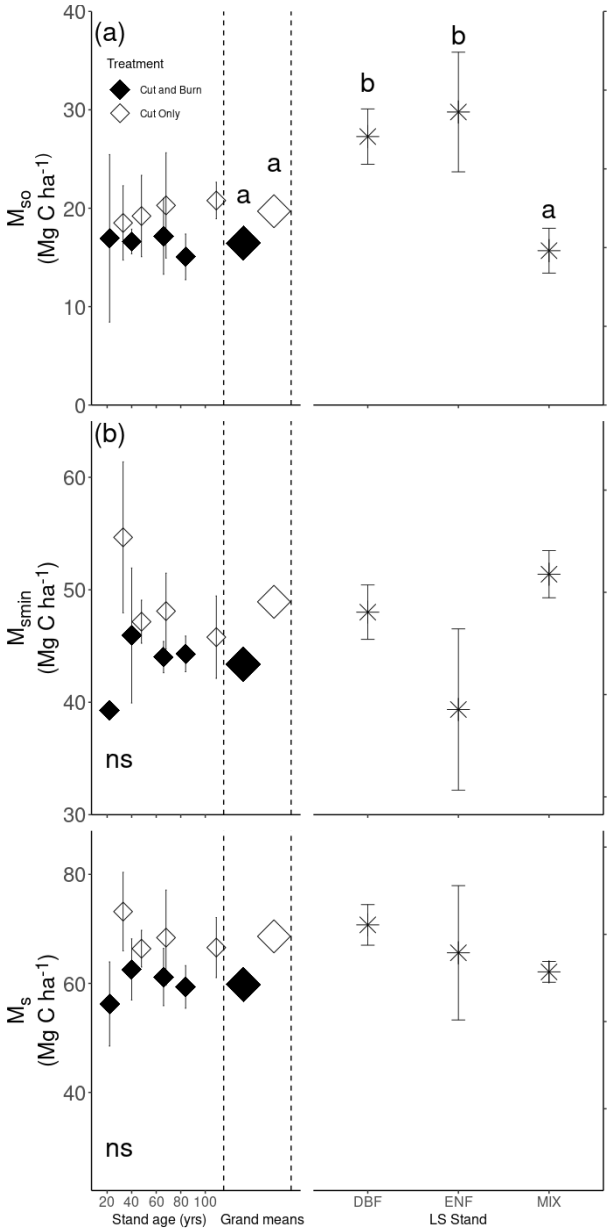

Figure 4: Soil O horizon, mineral horizon, and total soil carbon mass across stand age and late successional stands. Error bars represent +/- SE. Mean values with shared letters above them represent values that are statistically the same.

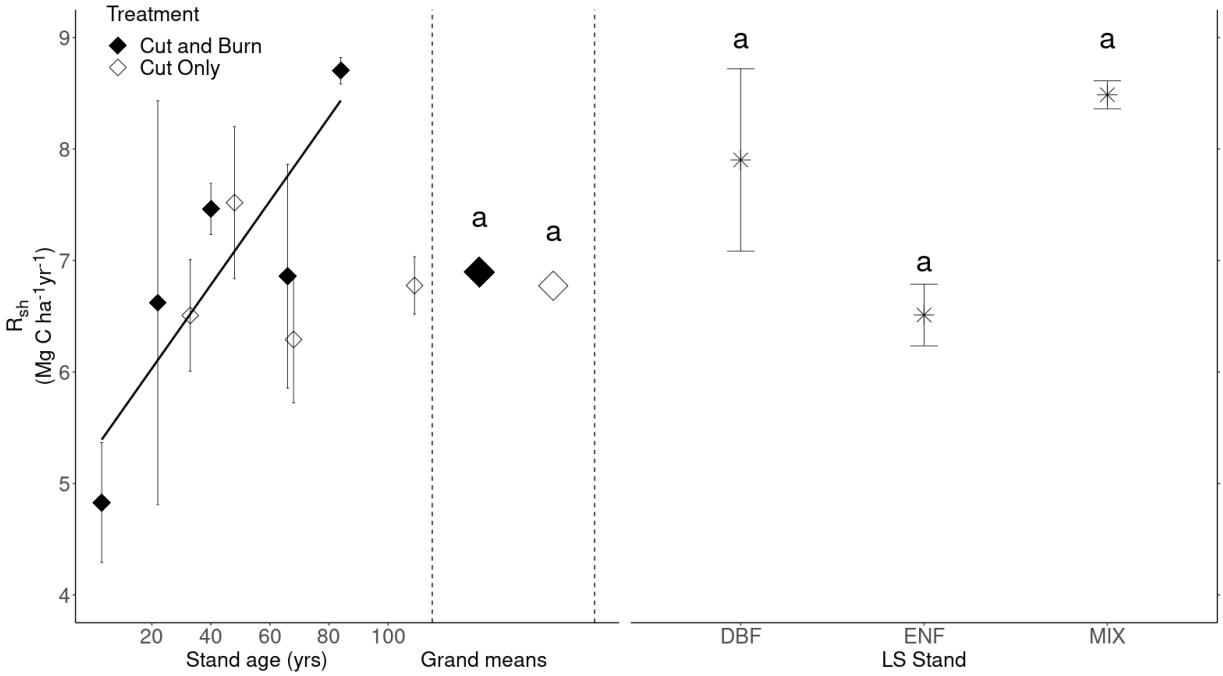

Figure 5: Heterotrophic soil respiration across stand age and late successional stands. Error presented represents variation between plots. Error bars represent the error region generated around each study site. Mean values with shared letters above them represent values that are statistically the same.

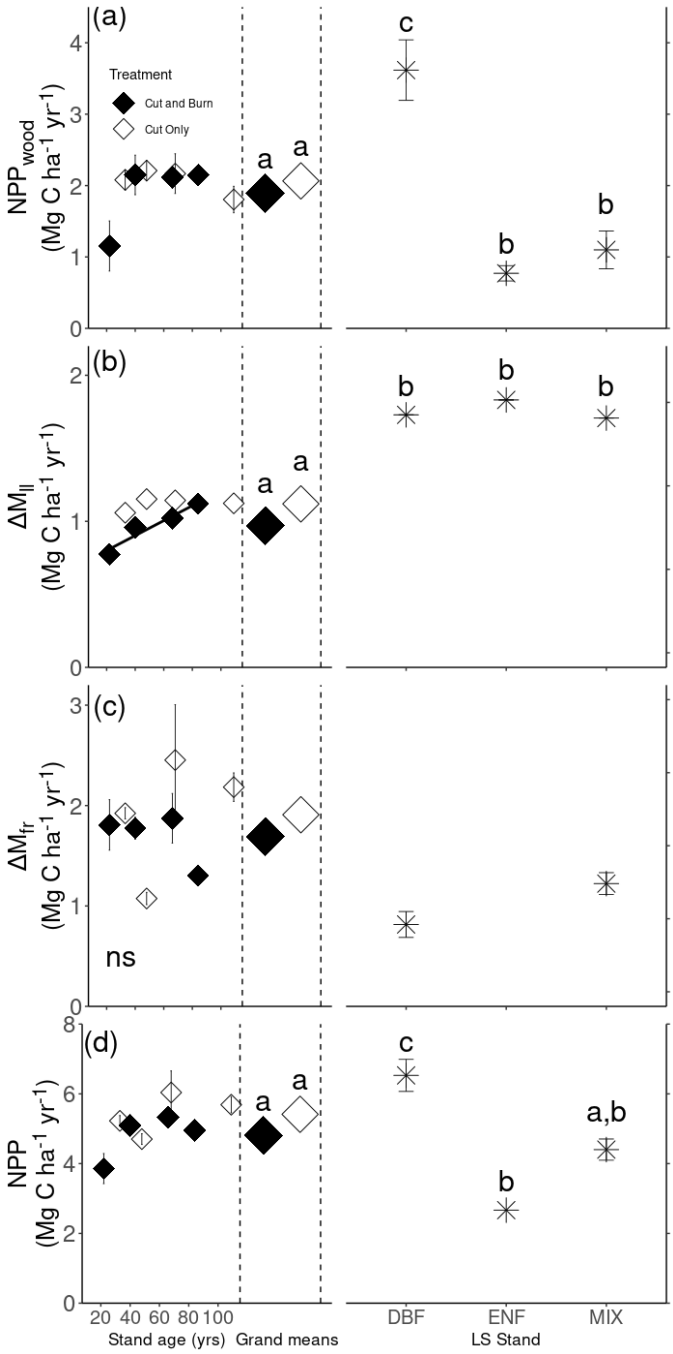

Figure 6: NPP and its components, Wood NPP, Fine Root NPP, and leaf/litter NPP, across stand age and late successional stands. The solid black line represents a slope for the high disturbance chronosequence that is non-zero. Fine root data was unavailable in the ENF late successional stand. Error bars represent +/- SE. Mean values with shared letters above them represent values that are statistically the same.

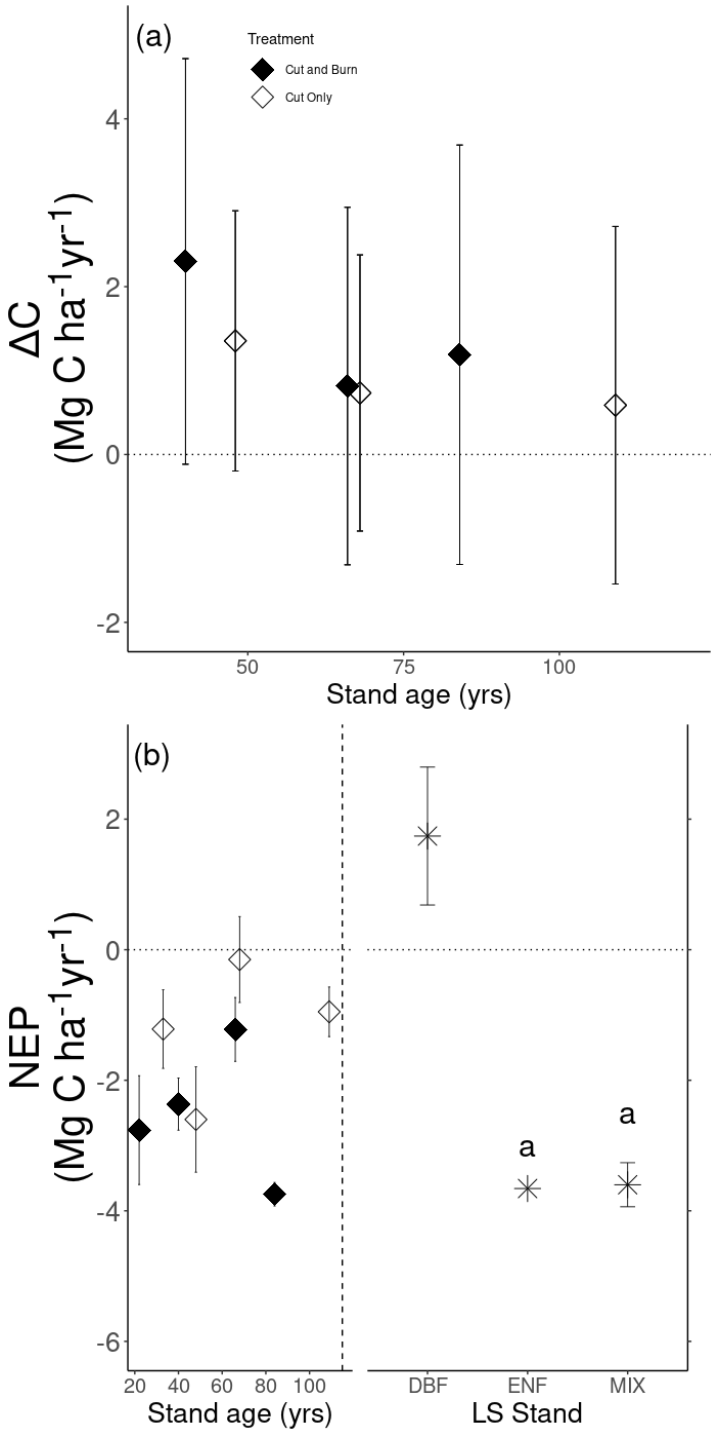

Figure 7: Change in carbon storage rate over time and between late successional stands, comparing the C increment (annual change in carbon pool size over time) to the NEP method (the sum of all carbon fluxes at each point in time). Error bars represent +/- SE. Mean values with shared letters above them represent values that are statistically the same.

	Cut and Burn				Cut Only				Reference Stands		
	Stand age (years)										
Category	22	40	66	84	33	48	68	109	ENF	DBF	MIX
C Pools (Mg C ha-1)											
M_a	12.84 (11.08)	42.47 (3.92)	59.85 (3.67)	80.5 (6.23)	34.13 (2.15)	55.63 (1.21)	67.05 (9.21)	88.28 (3.5)	123.83 (5.07)	201.07 (20.75)	120.34 (12.37)
M_{ll}	0.77 (0)	0.96 (0)	1.02 (0)	1.12 (0)	1.06 (0)	1.15 (0)	1.14 (0)	1.12 (0)	1.51 (0)	1.43 (0)	1.41 (0)
M_{fd}	0.12 (0)	0.21 (0)	0.32 (0)	0.39 (0)	0.16 (0)	0.27 (0)	0.27 (0)	0.58 (0)	0.38 (0)	0.56 (0)	0.41 (0)
M_{cwd}	1.27 (2.19)	0.8 (0.26)	2.55 (3.46)	0.97 (1.41)	1.14 (0.18)	2.45 (0.42)	1.39 (2.8)	1.81 (0.93)	1.67 (0.84)	25.14 (2.59)	3.24 (2.3)
M_{fr}	4.2 (1.33)	6.3 (0.8)	6.75 (1.88)	6.84 (1.18)	8.35 (0.14)	7.88 (0.86)	9.58 (1.68)	7.94 (0.29)	7.23 (1.44)	4.16 (0.68)	4.61 (0.67)
M_s	56.22 (19.63)	62.56 (4.83)	61.16 (13.37)	59.35 (9.94)	73.17 (6.2)	66.37 (2.9)	68.39 (22.2)	66.57 (4.75)	75.76 (13.25)	82.16 (4.01)	71.38 (2.05)
M_{so}	16.94 (21.64)	16.62 (1.08)	17.15 (9.82)	15.05 (5.9)	18.51 (3.25)	19.21 (3.56)	20.29 (13.61)	20.78 (1.6)	37.22 (6.54)	34.1 (3.02)	19.61 (2.45)
M_{smin}	39.28 (2)	45.94 (5.16)	44.01 (3.55)	44.3 (4.04)	54.66 (5.78)	47.16 (1.65)	48.1 (8.6)	45.79 (3.15)	38.54 (6.78)	48.06 (2.29)	51.77 (1.98)
C Fluxes (Mg C ha-1 yr-1)											
ΔM_{cwd}	-0.29 (0.04)	-0.13 (0.12)	0.3 (0.8)	-0.25 (0.32)	0.01 (0.08)	0.22 (0.11)	0.03 (0.44)	0 (0.19)	0.04 (0.22)	3.11 (0.1)	0.48 (0.38)
ΔM_{fr}	1.81 (0.64)	1.77 (0.09)	1.87 (0.63)	1.3 (0.26)	1.92 (0.05)	1.07 (0.05)	2.45 (1.41)	2.18 (0.12)	-	0.92 (0.15)	1.48 (0.13)
R_{sh}	-6.62 (1.81)	-7.46 (0.23)	-6.86 (1)	-8.7 (0.12)	-6.51 (0.5)	-7.52 (0.68)	-6.29 (0.57)	-6.78 (0.26)	-6.51 (0.28)	-7.9 (0.82)	-8.49 (0.13)
NPP_{wood}	1.15 (1.05)	2.15 (0.28)	2.11 (0.44)	2.15 (0.42)	2.08 (0.14)	2.21 (0.14)	2.17 (0.83)	1.8 (0.19)	0.77 (0.11)	3.62 (0.43)	1.1 (0.27)
Total Carbon Mass	78 (36.45)	121.79 (8.15)	143.62 (16.19)	165.27 (17.19)	124.83 (7.44)	144.87 (4.46)	161.24 (12.26)	183.97 (7.81)	235.15 (16.42)	354.73 (24.72)	225.46 (17.9)
NEP	-2.76 (0.12)	-2.36 (0.04)	-1.22 (0.4)	-3.75 (0.04)	-1.22 (0.51)	-2.6 (0.69)	-0.15 (1.4)	-0.95 (0.44)	-3.66 (0.44)	1.74 (0.3)	-3.6 (0.88)
NPP	3.86 (1.69)	5.1 (0.2)	5.33 (0.18)	4.96 (0.16)	5.23 (0.18)	4.7 (0.13)	6.04 (0.57)	5.69 (0.31)	2.67 (0.11)	6.53 (0.58)	4.4 (0.4)

Table 1. Ecosystem flux and pool values, represented in Mg C ha^{-1} (for pools) and Mg C ha^{-1} yr^{-1} (for fluxes).